

Tests of the Stokes-Einstein Relation through the Shear Viscosity Activation Energy of Water

Camina H. Mendis,¹ Zeke A. Piskulich,¹ and Ward H. Thompson^{1, a)}

Department of Chemistry, University of Kansas, Lawrence, KS 66045, USA

A method for calculating the activation energy for the shear viscosity of a liquid from simulations at a single temperature is demonstrated. Importantly, the approach provides a route to the rigorous decomposition of the activation energy into contributions due to different motions and interactions, *e.g.*, kinetic, Coulombic, and Lennard-Jones energies, that are otherwise not accessible. The method is illustrated by application to the case of liquid water under ambient conditions. The shear viscosity activation energy and its components are examined and compared to the analogous results for the timescales of diffusion and reorientation that have been previously calculated, providing a test of the Stokes-Einstein relation for water.

I. INTRODUCTION

Water plays a fundamental role as a solvent in systems ranging from industrial catalysis to fuel cells to the biological milieu.^{1–6} Its dynamical properties are as important to processes in these environments as its phase and solvation characteristics. In particular, the timescales of water motions, *e.g.*, diffusion, reorientation, and hydrogen-bond (H-bond) exchange, can influence or determine the rates of physical and chemical transformations.^{7–9}

Central among the dynamical properties of water are the transport coefficients that link macroscopic characteristics and molecular behavior. The shear viscosity, η_s , is a key example, as its magnitude can even be examined visually in the flow of the liquid while it can also be used to predict timescales for molecular motion such as diffusion through the Stokes-Einstein relation,¹⁰ *e.g.*,

$$D = \frac{k_B T}{C \pi r \eta_s}. \quad (1)$$

Here, D is the diffusion coefficient, k_B Boltzmann's constant, T the temperature, r the hydrodynamic radius of the diffusing particle, and C is a factor that is 4 or 6 for slip or stick boundary conditions for diffusion, respectively.

Beyond predicting the rate of translational motion for a molecule in a liquid (D) from the viscosity, Eq. 1 also provides a route to the temperature dependence. This is typically measured by the activation energy,

$$E_{a,D} = -\frac{\partial \ln D(T)}{\partial \beta}, \quad (2)$$

where $\beta = 1/k_B T$. By definition, $E_{a,D}$ measures how D changes with T , however, it has a further mechanistic interpretation if one assumes that the temperature dependence is due to an underlying barrier that must be surmounted for diffusion to occur. Then, $E_{a,D}$ is related to the height of that energetic barrier or, equivalently,^{11,12}

the energy that the system must have for the diffusing particle to pass over the barrier. The Stokes-Einstein relation indicates that the activation energy for diffusion is directly related to that for $1/\eta_s$, the fluidity, with the implication that they are both determined by the same barrier at the molecular level.

In the case of water, both D and $1/\eta_s$ are well known to exhibit significantly non-Arrhenius behavior,^{13–16} *i.e.*, their activation energies are not constant and as the temperature is reduced both quantities decrease more rapidly in magnitude. This makes calculation of their activation energies challenging. The standard approach is to calculate, *e.g.*, η_s , at multiple temperatures above and below the one of interest, then $E_{a,1/\eta_s}$ is obtained from the negative of the slope of an Arrhenius plot of $1/\eta_s(T)$ versus β . The non-Arrhenius behavior of $1/\eta_s$ means that the value of $E_{a,1/\eta_s}$ from such an analysis depends on the temperatures used. Ideally the temperatures would be as close as possible to the T of interest, however, resolving the changes in η_s over a narrow temperature range is difficult for both experiments and simulations.

In this Paper, we present an approach for directly obtaining the activation energy of the shear viscosity from simulations at a single temperature that extends previous work on other dynamical timescales.^{17–21} The method calculates the analytical derivative of $1/\eta_s$ with respect to β in contrast to the numerical derivative approximation intrinsic to the Arrhenius analysis. Most importantly, it provides a way to decompose the activation energy into the different contributions from components of the system energy, effectively giving the amount of each type of energy that is required to surmount the underlying barrier for the process. We apply this method to the shear viscosity of water and compare it to analogous results for the diffusion coefficient¹⁹ and reorientation times.²¹ Such an analysis thus provides new insight into the Stokes-Einstein relation and the mechanisms associated with both diffusion and viscosity.

^{a)} Electronic mail: wthompson@ku.edu

II. THEORY

The shear viscosity η_s can be calculated from the Green-Kubo (GK) relation,

$$\begin{aligned}\eta_s &= \frac{V}{k_B T} \int_0^\infty \langle P_{\alpha\beta}(0) P_{\alpha\beta}(t) \rangle dt \\ &\equiv \beta V \int_0^\infty C_{\eta_s}(t) dt,\end{aligned}\quad (3)$$

where V is the simulation box volume and the angle brackets indicate a thermal ensemble average. Here, the repeated $\alpha\beta$ subscript denotes an average of the five autocorrelation functions constructed from the anisotropic terms of the stress tensor: P_{xy} , P_{yz} , P_{xz} , $(P_{xx}-P_{yy})/2$, and $(P_{yy}-P_{zz})/2$.

The expression for the viscosity given in Eq. 3 is a particular example of the GK relations that give a transport coefficient σ in terms of the Fourier transform or integral of a time correlation function (TCF) of the general form

$$\sigma(\omega) = \int_0^\infty e^{-i\omega t} \langle \dot{A}(0) \dot{B}(t) \rangle dt. \quad (4)$$

Here, A and B are functions of the phase space variables and the transport coefficient is, in general, a function of the frequency ω of the applied field. The isothermal-isobaric (NPT) ensemble average can be expressed in more detail as

$$\begin{aligned}\langle \dot{A}(0) \dot{B}(t) \rangle &= \frac{1}{\Delta h^F} \int d\mathbf{p}_0 \int d\mathbf{q}_0 e^{-\beta[H(\mathbf{p}_0, \mathbf{q}_0) + PV(0)]} \\ &\times \dot{A}[\mathbf{p}_0, \mathbf{q}_0] \dot{B}[\mathbf{p}(t), \mathbf{q}(t)],\end{aligned}\quad (5)$$

where H is the Hamiltonian, \mathbf{p} and \mathbf{q} the system momenta and positions (\mathbf{p}_0 and \mathbf{q}_0 at $t = 0$), F the number of degrees-of-freedom, h Planck's constant, and Δ the isothermal-isobaric partition function. Then the only temperature-dependent factors in $\sigma(\omega)$ are Δ and the Boltzmann factor. This gives the temperature derivative as

$$\frac{\partial \langle \dot{A}(0) \dot{B}(t) \rangle}{\partial \beta} = -\langle [H(0) + PV(0)] \dot{A}(0) \dot{B}(t) \rangle + \frac{1}{\Delta} \frac{\partial \Delta}{\partial \beta}. \quad (6)$$

The second term can be identified as the negative of the average enthalpy, $\langle H \rangle + P\langle V \rangle$, so that

$$\frac{\partial \langle \dot{A}(0) \dot{B}(t) \rangle}{\partial \beta} = -\langle [\delta H(0) + P\delta V(0)] \dot{A}(0) \dot{B}(t) \rangle, \quad (7)$$

where $\delta H(0) = H(0) - \langle H \rangle$ is the fluctuation of the energy at $t = 0$ from its average value and similarly $\delta V(0) = V(0) - \langle V \rangle$. This is a general expression for any GK time correlation function at constant temperature and pressure.

Then the activation energy for the transport coefficient

can then be expressed as

$$\begin{aligned}E_{a,\sigma} &= -\frac{\partial \ln \sigma(\omega)}{\partial \beta} \\ &= \frac{\int_0^\infty e^{-i\omega t} \langle [\delta H(0) + P\delta V(0)] \dot{A}(0) \dot{B}(t) \rangle dt}{\int_0^\infty e^{-i\omega t} \langle \dot{A}(0) \dot{B}(t) \rangle dt}.\end{aligned}\quad (8)$$

Note that this gives the activation energy in terms of TCFs that are evaluated at a single temperature. Fundamentally, this approach is statistical mechanical fluctuation theory applied to dynamics. Applied to the case of the inverse viscosity, $1/\eta_s$, this gives

$$\begin{aligned}E_{a,1/\eta_s} &= k_B T - \frac{\int_0^\infty \langle [\delta H(0) + P\delta V(0)] P_{\alpha\beta}(0) P_{\alpha\beta}(t) \rangle dt}{\int_0^\infty \langle P_{\alpha\beta}(0) P_{\alpha\beta}(t) \rangle dt} \\ &= k_B T + \frac{\int_0^\infty C_{H,\eta_s}(t) dt}{\int_0^\infty C_{\eta_s}(t) dt},\end{aligned}\quad (9)$$

where the last equality, together with Eq. 3, defines the weighted TCF $C_{H,\eta_s}(t)$. We choose to calculate the activation energy for $1/\eta_s$ instead of η_s because $E_{a,1/\eta_s}$ is positive.

For water under ambient conditions, the term involving the volume fluctuations, which gives the contribution to $E_{a,1/\eta_s}$ due to the activation volume of the viscosity, is three or four orders-of-magnitude smaller than that from the energy and can be neglected without loss of accuracy. Thus, in the following we use $C_{H,\eta_s}(t) = -\langle \delta H(0) P_{\alpha\beta}(0) P_{\alpha\beta}(t) \rangle$.

III. COMPUTATIONAL DETAILS

The activation energy for the shear viscosity of water has been calculated according to Eq. 9. Twenty separate 50 ns trajectories starting from different initial equilibrium configurations were propagated in the isobaric-isothermal (NPT) ensemble. Each trajectory was used to obtain 50,000 initial configurations and velocities for subsequent NVE simulations, from which the shear correlation function and its derivative were calculated. These configurations sample the Gaussian distribution of energies and volumes, $\delta H(0)$ and $\delta V(0)$, explored by the NPT trajectory and provide a total of 1,000,000 configurations representative of $T = 298.15$ K and $P = 1$ bar.

The MD simulations were performed using the Large-Scale Atomic/Molecular Massively Parallel Simulator (LAMMPS).^{22,23} A bulk water system of 343 TIP4P/2005 water molecules was used due to the ability of the TIP4P/2005 model to accurately describe the temperature dependence of water transport properties.²⁴ The water molecules were kept rigid using the SHAKE algorithm with a tolerance of 1.0×10^{-4} which was confirmed to give good energy conservation.²⁵ The TIP4P/2005 model is a four-site model that incorporates a fourth charge off of the oxygen atom that improves the electrostatic treatment of water compared with other commonly

used water models. Electrostatic interactions were calculated with the Particle Particle Mesh (PPPM) method,^{26–28} with an accuracy parameter of 1.0×10^{-4} . The Lennard-Jones (LJ) interaction cutoff was 10.5 Å, while the division between electrostatic calculations in real and k -space was at 8.5 Å.

In the NPT trajectories a three-chain Nosé-Hoover thermostat was employed with a 100 fs damping parameter and the barostat damping parameter was 1 ps. The dynamics are evaluated from 1,000,000 separate 50 ps NVE trajectories launched at 1 ps intervals throughout the long trajectories. As shown below, these trajectories need not be longer than ~ 6 ps for the present purposes; longer trajectories were used for a different analysis not discussed here. A 1 fs timestep was used for all simulations, and pressures were calculated every 10 fs from the NVE trajectories. Simulations were divided into 5 blocks of 200,000 trajectories each for block averaging to obtain 95% confidence intervals according to the Student's t -distribution,²⁹ which are the errors reported on the data.

An Arrhenius analysis was carried out by simulations using the same method at 280 and 320 K. In these cases, a single 50 ns NPT trajectory was used to generate 50,000 NVE trajectories of 50 ps each. We note that this approach is more efficient for obtaining $E_{a,1/\eta_s}$ than the present method, but cannot provide the energetic decomposition of the activation energy. This is in contrast to previous work on diffusion and reorientation dynamics,^{19–21} and reflects the challenges of converging transport coefficients through Green-Kubo TCFs. More recently developed non-equilibrium approaches for calculating the shear viscosity^{30,31} represent a more promising path for efficient calculations of the activation energy if the present method can be extended to them.

IV. RESULTS

A. Viscosity

We have calculated the shear viscosity using the simulations described in the previous section based on the stress tensor time correlation function $C_{\eta_s}(t)$, Eq. 3. This TCF is shown in Fig. 1 as a function of time. It displays a sharp initial decay in less than 50 fs followed by several oscillations with a period of 120 fs, which are damped out in less than a picosecond. It then exhibits a longer timescale decay with a time constant of 0.85 ps, which is complete in less than 3 ps.

The shear viscosity is related to the integral of this TCF, which is also plotted in Fig. 1. The integral reaches a plateau after ~ 4 ps that is maintained for the remainder of the 50 ps simulation time used in computing the TCFs. The calculated numerical integral gives the shear viscosity as 0.768 ± 0.008 cP at 298.15 K from the integral Eq. 3 with an upper time limit of 6 ps. There have been several previous calculations of the shear viscosity of wa-

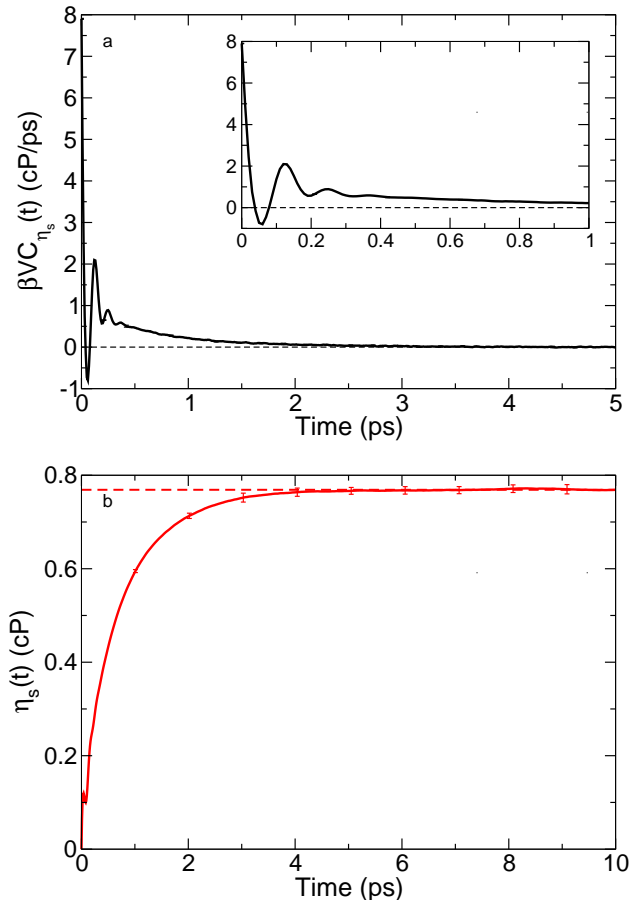


FIG. 1: The stress tensor TCF, $C_{\eta_s}(t)$, (solid black line) is shown along with its integral (solid red line) as a function of time. The integral equals the shear viscosity, η_s , at long times (dashed red line).

ter using a variety of force fields.^{32–41} Several studies have considered the TIP4P/2005 model used here and obtained values of $\eta_s = 0.78$,³⁹ 0.807,³⁷ 0.82,⁴¹ 0.83,³⁶ 0.855,³³ and 0.89 cP.⁴² The measured shear viscosity is 0.8903 cP.¹⁶ Our result is generally smaller than the values obtained in these previous simulations and measurements. The key difference is that our result is obtained for the NPT ensemble which gives an average density of 0.987 g/cm³ in our simulations, which, due to our choice of long-range tail corrections, is lower than the densities of 0.998–1.00 g/cm³ used in the other simulations.

B. Activation Energy

The activation energy of the inverse shear viscosity, $1/\eta_s$, can be calculated as $k_B T$ plus the ratio of the integrated time correlation function weighted by the energy fluctuation, $C_{H,\eta_s}(t)$, and the integral of the unweighted TCF, $C_{\eta_s}(t)$, Eq. 9. The weighted TCF $C_{H,\eta_s}(t)$ is shown in Fig. 2a. It exhibits a rise at times less than 0.5 ps which is modulated by an oscillation of period ~ 100 fs,

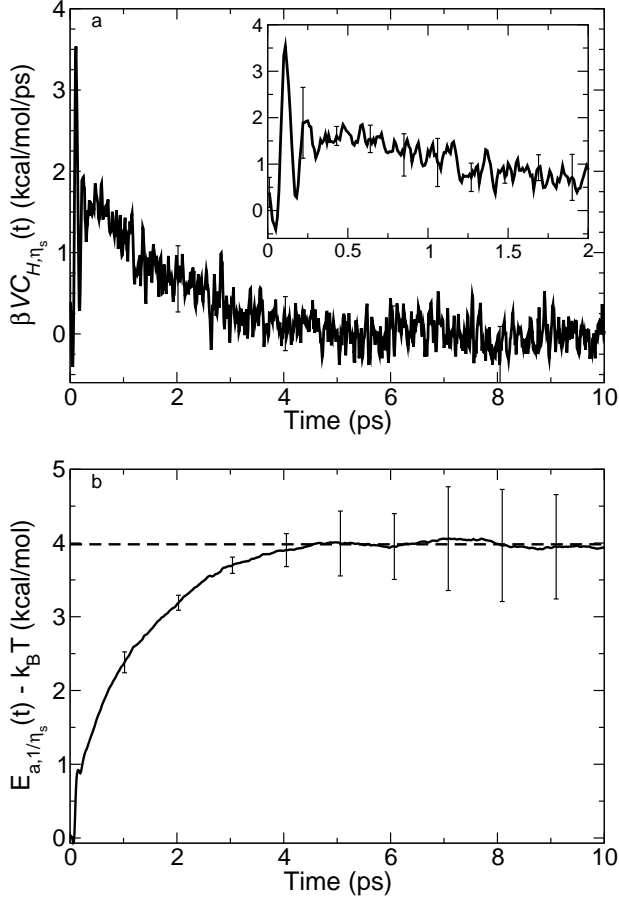


FIG. 2: (a) Weighted shear viscosity TCF, $C_{H,\eta_s}(t)$, plotted versus time (solid black line). The short-time behavior is shown in the inset. (b) Ratio of the integrals of $C_{H,\eta_s}(t)$ and $C_{\eta_s}(t)$ as a function of the upper integration limit time (solid black line). This equals $E_{a,1/\eta_s} - k_B T$ at long times (dashed black line).

followed by a decay over a longer timescale of ~ 1.8 ps.

The weighted-to-unweighted ratio of the integrated TCFs in Eq. 9 is shown as a function of the time used for the upper limit of integration in Fig. 2b. The ratio reaches a stable plateau at longer times ($t > 4$ ps), which gives the activation energy for $1/\eta_s$ within $k_B T$. The activation energy value is obtained from the ratio at 6 ps, yielding $E_{a,1/\eta_s} = 3.94 \text{ kcal/mol} + k_B T = 4.53 \pm 0.45 \text{ kcal/mol}$. This is in excellent agreement with an Arrhenius analysis based on calculation of η_s at 280 and 320 K, which gives $E_{a,1/\eta_s}^{Arr} = 4.53 \text{ kcal/mol}$. This accord indicates that the shear viscosity activation energy is most efficiently obtained from an Arrhenius approach; the advantage of the direct method presented here is the mechanistic insight it provides, as discussed in the next section.

We have obtained the experimental activation energy by fitting the temperature-dependent experimental inverse viscosities, $1/\eta_s$, given in Ref. 16 to a cubic function in β and using this functional form to evaluate the activation energy at 298.15 K; the experimental $1/\eta_s$

shows significant non-Arrhenius behavior over the temperature range 273 – 373 K, requiring the higher order fit. (An Arrhenius analysis still represents a good local approximation, but this approach eliminates any dependence on the choice of temperature range.) The result of this analysis is an experimental activation energy of $E_{a,1/\eta_s}^{expt} = 4.03 \text{ kcal/mol}$, which is lower than the calculated result. Other reports give $E_{a,1/\eta_s}^{expt} = 4.02$ and 4.05 kcal/mol .^{13–15}

C. Energy Decomposition

Previous studies using this direct method of calculating activation energies of diffusion coefficient and reorientation times have shown that the E_a associated with these dynamical processes can be decomposed into specific contributions from various components of the total energy.^{19,21} We have applied the same approach to the shear viscosity activation energy. The fluctuation in total energy can be written as,

$$\delta H(0) = \delta KE(0) + \delta U_{LJ}(0) + \delta U_{Coul}(0), \quad (10)$$

where $\delta KE(0)$, $\delta U_{LJ}(0)$, and $\delta U_{Coul}(0)$ are the fluctuations in the kinetic, Lennard-Jones (LJ), and Coulombic energies, respectively. Within the fixed-charge, pairwise TIP4P/2005 force field used in the present simulations, this is an exact expression.

Then the total shear viscosity activation energy can be decomposed as

$$E_{a,1/\eta_s} = k_B T + E_{a,1/\eta_s}^{KE} + E_{a,1/\eta_s}^{LJ} + E_{a,1/\eta_s}^{Coul}. \quad (11)$$

Each of the terms on the right-hand-side of this equation is a component of the activation energy associated with the fluctuations of a particular component of the total system energy, obtained by substituting Eq. 10 into Eq. 9 (with the volume fluctuations neglected). In the case of the Lennard-Jones contribution, this gives

$$\begin{aligned} E_{a,1/\eta_s}^{LJ} &= -\frac{\int_0^\infty \langle \delta U_{LJ}(0) P_{\alpha\beta}(0) P_{\alpha\beta}(t) \rangle dt}{\int_0^\infty \langle P_{\alpha\beta}(0) P_{\alpha\beta}(t) \rangle dt}, \\ &= \frac{\int_0^\infty C_{LJ,\eta_s}(t) dt}{\int_0^\infty C_{\eta_s}(t) dt}, \end{aligned} \quad (12)$$

where $C_{LJ,\eta_s}(t) = -\langle \delta U_{LJ}(0) P_{\alpha\beta}(0) P_{\alpha\beta}(t) \rangle$ is the contribution to $C_{H,\eta_s}(t)$ from the Lennard-Jones interactions. The components associated with the kinetic energy, $E_{a,1/\eta_s}^{KE}$, and Coulombic interactions, $E_{a,1/\eta_s}^{Coul}$, can be calculated in an analogous way.

The kinetic, Lennard-Jones, and Coulombic energy contributions to the activation energy are shown in Fig. 4 and given in Table I. The total activation energy is provided for comparison. In Fig. 4, the ratio for each activation energy component is shown as a function of the upper integration limit. These ratios converge to constant values in ~ 4 ps and we use the value at 6 ps to compute the activation energy contributions.

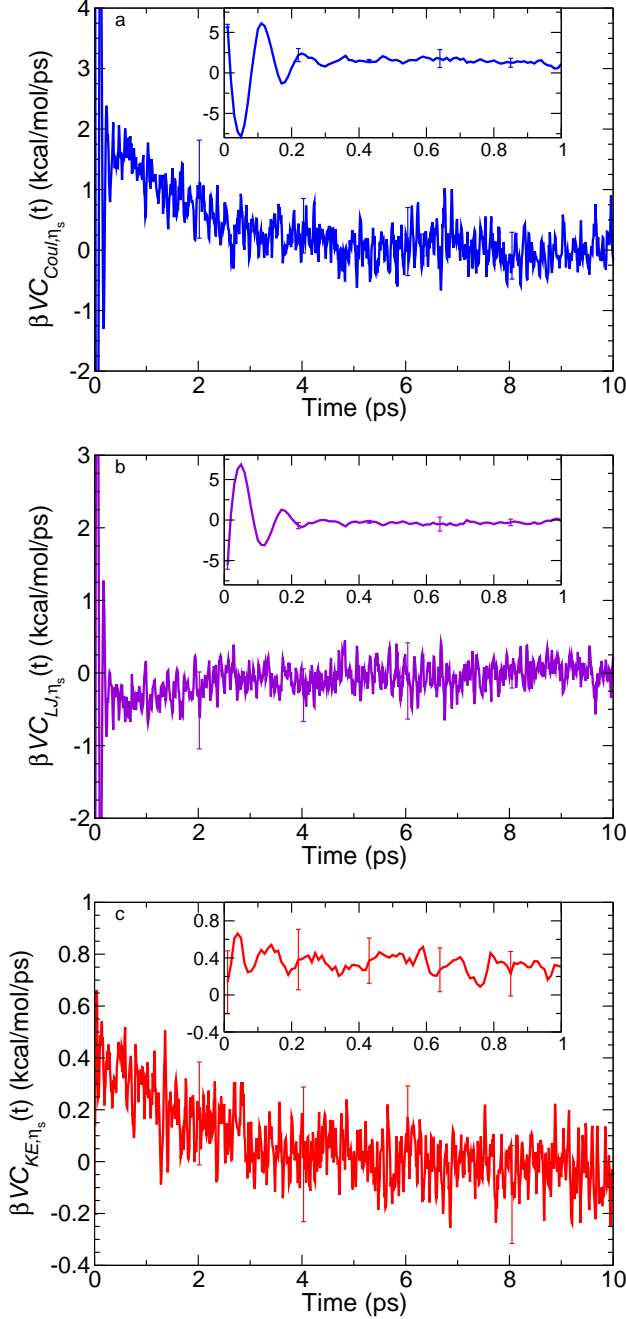


FIG. 3: The stress tensor correlation function, $\beta VC_{X,\eta_s}(t)$, weighted by the (a) Coulombic potential energy (blue), (b) Lennard-Jones potential energy (violet), and (c) kinetic energy (red). Insets show the short-time behavior.

These contributions to the shear viscosity activation energy can be understood in the context of Tolman's interpretation of the activation energy.^{11,12} He showed that the activation energy for a chemical reaction can be understood as the average energy of reacting species, $\langle E \rangle_{\text{reacting}}$ minus the average energy of the reactants, $\langle E \rangle$, so that $E_a = \langle E \rangle_{\text{reacting}} - \langle E \rangle$. In this context, E_a measures the energy required to overcome the bar-

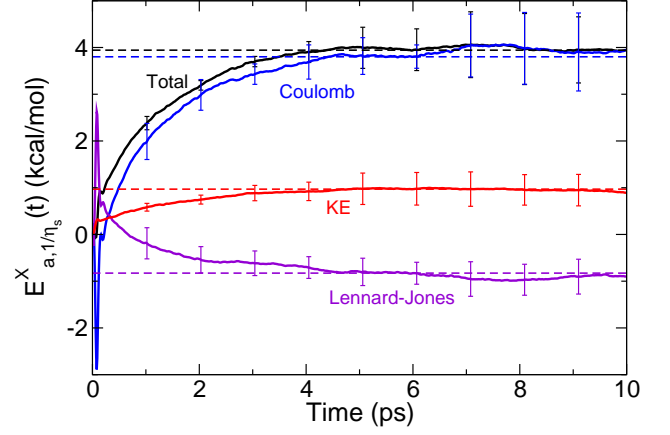


FIG. 4: Contributions to the $1/\eta_s$ activation energy due to Coulombic (blue) and Lennard-Jones (violet) interactions and kinetic energy (red) compared to the total result (black). In each case the integral of $C_{X,\eta_s}(t)$, $X = KE, LJ$, and $Coul$, divided by the integral of $C_{\eta_s}(t)$ is shown as a function of the upper integration limit (solid lines); dashed lines indicate the values at 6 ps.

rier to reaction and each contribution is then the amount of required energy in a given motion (kinetic energy) or interaction (potential energy). For the shear viscosity, the nature of the barrier is not well defined as it is in the case of a chemical reaction. That is, it is not clear how to define a reaction coordinate that takes the system over the barrier. However, several analyses support the notion that for water it is closely related to the exchange of H-bonds^{41,43} and the similarity of the activation energy to that for diffusion (*vide infra*), reorientation,^{19,21} and H-bond exchange itself^{44,45} supports this conclusion.

The activation energy decomposition shows that the electrostatic interactions are the dominant contribution to $E_{a,1/\eta_s}$ with a value, $E_{a,1/\eta_s}^{Coul} = 3.80$ kcal/mol, that is nearly identical to the total result of 3.94 kcal/mol for the TCF component. This is a result of a nearly complete cancellation between the kinetic energy and Lennard-Jones contributions. Namely, while the kinetic energy component of the activation energy is positive, $E_{a,1/\eta_s}^{KE} = 0.97$ kcal/mol, the Lennard-Jones term is negative, $E_{a,1/\eta_s}^{LJ} = -0.83$ kcal/mol. These results indicate that $1/\eta_s$ decreases, *i.e.*, the water shear viscosity is enhanced, by fluctuations that increase the Lennard-Jones interaction energy in the system, while the reverse is true for the electrostatic and kinetic energy. Or, equivalently, the shear viscosity is decreased most by increases in the Coulombic interaction energy.

Act. Ener.	$1/\eta_s$	D_{PBC}	τ_2	$\langle\tau_2\rangle$
E_a^{total}	4.53 ₄₅	4.267 ₉	4.28 ₁₀	4.58 ₁₁
E_a^{LJ}	-0.83 ₂₅	-1.363 ₂₀	-1.31 ₆	-1.54 ₇
E_a^{Coul}	3.80 ₂₅	4.436 ₈₈	4.38 ₁₃	4.98 ₁₄
E_a^{KE}	0.97 ₃₅	1.194 ₃	1.21 ₄	1.14 ₄
$k_B T$	0.59	—		

TABLE I: Total activation energy and the contributions due to the kinetic energy (KE) and Lennard-Jones (LJ) and Coulombic (Coul) interactions for the shear viscosity, $1/\eta_s$, diffusion coefficient from the periodic boundary conditions simulations, D_{PBC} , reorientation time, τ_2 , and integrated reorientation time, $\langle\tau_2\rangle$. Data for τ_2 and $\langle\tau_2\rangle$ are taken from Ref. 21. All values are in kcal/mol; subscripts indicate uncertainties in the trailing digits.

V. DISCUSSION

A. Comparison with the Molecular-level Timescales

We have previously shown how the activation energies of the diffusion coefficient, D , and reorientation times can also be obtained from simulations at a single temperature.^{19,21} Briefly, considering D as an example, it is obtained from the mean-squared displacement, MSD , as

$$D = \lim_{t \rightarrow \infty} \frac{\langle |\vec{r}(t) - \vec{r}(0)|^2 \rangle}{6t} = \lim_{t \rightarrow \infty} \frac{MSD(t)}{6t}, \quad (13)$$

where $\vec{r}(t)$ is the position vector of the species of interest (here the water center-of-mass) at time t and the average is over all molecules. By taking the derivative of D with respect to β in analogy to Eq. 6, one can show that¹⁹

$$\begin{aligned} E_{a,D} &= \frac{\lim_{t \rightarrow \infty} \langle [\delta H(0) + P\delta V(0)] |\vec{r}(t) - \vec{r}(0)|^2 \rangle}{\lim_{t \rightarrow \infty} \langle |\vec{r}(t) - \vec{r}(0)|^2 \rangle} \\ &= \frac{\lim_{t \rightarrow \infty} MSD_H(t)}{\lim_{t \rightarrow \infty} MSD(t)}. \end{aligned} \quad (14)$$

In practice we calculate the slope of both $MSD_H(t)$ and $MSD(t)$ at long times and take the ratio to obtain the activation energy. Similar expressions have been obtained for the OH reorientation times in water. Particularly we have shown how the longest decay timescale, τ_2 , of the reorientational TCF $C_2(t) = \langle P_2[\vec{e}_{OH}(0) \cdot \vec{e}_{OH}(t)] \rangle$ and the average reorientational time, $\langle\tau_2\rangle = \int_0^\infty C_2(t)dt$, can be obtained by an analogous approach.

The results obtained for the diffusion coefficient and reorientation time activation energies and their decomposition into kinetic, Coulombic, and Lennard-Jones energy components are given in Table I. The reorientation time data are taken from Ref. 21. The diffusion coefficient values are calculated from the same trajectories described in ‘‘Computational Methods’’ that were used to evaluate η_s and its activation energy; the diffusion results are better determined, however, since each water molecule contributes separately to the averaging. The

value of the diffusion coefficient is known to be sensitive to the size of the periodic boundary condition simulation box,^{46,47} as

$$D = D_{PBC} + \frac{2.837297 k_B T}{6\pi\eta_s L}, \quad (15)$$

where D_{PBC} is the value calculated with a simulation box of length L and D is the diffusion coefficient in an infinite system. The present simulations give $D = 2.382 \times 10^{-5} \text{ cm}^2/\text{s}$ after applying this correction. This is in good agreement with the accepted best value from measurements of $2.229 \times 10^{-5} \text{ cm}^2/\text{s}$.^{15,48–52} Interestingly, within the Stokes-Einstein approximation (see the Appendix) the correction for finite-size effects in Eq. 15 yields the same activation energy for D and D_{PBC} , so no adjustment is required for $E_{a,D}$. If the Stokes-Einstein relation is not assumed, Eq. 18 can be used to obtain the ‘‘corrected’’ activation energy for D and gives $E_{a,D} = 4.40 \pm 0.08 \text{ kcal/mol}$, which is only $0.13 \pm 0.08 \text{ kcal/mol}$ larger than $E_{a,D_{PBC}}$, indicating that these corrections are small.

B. Tests of the Stokes-Einstein Relation

We now use the comparison of the temperature dependence of η and the diffusion coefficient to investigate the validity of the Stokes-Einstein relation for water, Eq. 1. Specifically, we consider three approaches that focus on different predictions: 1) examining the ratio of $D\eta_s/T$ as a function of temperature, 2) comparing the activation energy values for D and η_s , and 3) analyzing the contributions to each activation energy due to the Coulombic, Lennard-Jones, and kinetic energies.

1. Is $D\eta_s/T$ Constant?

An approach that has been used extensively is to examine how the ratio $D\eta_s/T$ varies with temperature or density given that the Stokes-Einstein relation, Eq. 1, predicts it is constant. From our calculations at different temperatures, we find that $D\eta_s/T$ is nearly identical at 280 and 298.15 K with values of $6.11 \times 10^{-15} \text{ N/K}$ and $6.14 \times 10^{-15} \text{ N/K}$, respectively, but it is $\sim 15\%$ lower, $5.22 \times 10^{-15} \text{ N/K}$, at 320 K.

In contrast, Krynicki *et al.* found a constant value within experimental errors of $D\eta_s/T = 6.9 \pm 0.4 \times 10^{-15} \text{ N/K}$ over a wide range of temperatures based on their diffusion coefficient measurements and literature viscosity data.¹⁵ Other work by Woolf¹⁴ and Wilbur *et al.*⁵³ found that for H_2O and D_2O , respectively, that the ratio is effectively independent of density but decreases weakly with temperature, particularly above $\sim 305 \text{ K}$. These latter observations appear to be consistent with the present results. Wilbur *et al.* analyzed their results in terms of the boundary conditions implicit in the Stokes-Einstein equation, by calculating the factor

of $C = k_B T / (\pi r D \eta_s)$ in the denominator of Eq. 1 for different temperatures. They found that C increased from ~ 4.9 at 298 K to more than 6 at high temperatures, indicating that the boundary conditions for water molecule diffusion become more "stick"-like as temperature increases.

2. Stokes-Einstein Activation Energy Predictions

The Stokes-Einstein relation also directly links the activation energy for diffusion to that governing viscosity or, more directly, the inverse shear viscosity, $1/\eta_s$. Specifically, Eq. 1 predicts a direct relationship between the two as

$$E_{a,D} = E_{a,1/\eta_s} + k_B T. \quad (16)$$

Note that this can be obtained by setting the derivative of $D\eta_s/T$ with respect to β equal to zero and thus is formally equivalent to the above analysis of that ratio. However, Eq. 16 can be used to test the Stokes-Einstein relation at a single temperature, which the $D\eta_s/T$ ratio cannot, and is therefore represents a clearer evaluation.

Examination of the activation energies in Table I shows that the relation in Eq. 16 is not satisfied. From our calculated $E_{a,D}$, we would predict from the Stokes-Einstein relation that the $1/\eta_s$ activation energy is 3.675 ± 0.009 kcal/mol, which differs significantly from our calculated $E_{a,1/\eta_s} = 4.53 \pm 0.45$ kcal/mol. This suggests that for the TIP4P/2005 model, the temperature dependence implicit in the Stokes-Einstein relation is not quantitatively satisfied.

One approach to interpreting these apparent deviations from Stokes-Einstein behavior is to assume that Eq. 1 remains valid but that the hydrodynamic radius r is temperature dependent (and C is not). Then, it is straightforward to show that

$$\frac{\partial \ln r}{\partial \beta} = E_{a,D} - E_{a,1/\eta_s} - k_B T. \quad (17)$$

The data in Table I then gives $\partial \ln r / \partial \beta = -0.86$ kcal/mol at room temperature. Importantly, this indicates that if the Stokes-Einstein equation is assumed to hold, the hydrodynamic radius must increase with temperature, *i.e.*, $\partial r / \partial T > 0$. For water, the effective radius is related to the H-bonding structure and thus this interpretation suggests that the changes in the water H-bond network with temperature may influence the diffusion activation energy in a way that is independent of the viscosity.

An intriguing perspective is offered by the work of Eyring and co-workers,⁵⁴ who developed a theory of diffusion as a rate process. This yields a Stokes-Einstein-like relation in which the hydrodynamic radius, r , is replaced by a distance λ that measures the displacement a molecule undergoes between two equilibrium positions in the liquid, *i.e.*, it assumes D is determined by the same

H-bond exchanges as $1/\eta_s$ but their effect is weighted by the distance moved as a result of each exchange. In the case of water, we can envision this as the movement from one solvation shell to the next *via* H-bond exchanges. Within this interpretation, $\partial \lambda / \partial T > 0$ indicates that the distance between solvation shells increases with temperature, which is at least consistent with the known decreasing density of water with temperature above 4°C.⁵⁵

3. Comparison of Activation Energy Components

A comparison of the decomposition of the D , τ_2 , $\langle \tau_2 \rangle$, and $1/\eta_s$ activation energies provides additional insight. We first note that the activation energy components for D and τ_2 are identical (within errors), indicating that they are both governed by the same H-bond exchange dynamics. We have previously identified the origin of differences in the activation energies for τ_2 and the integrated reorientation time $\langle \tau_2 \rangle$ as the temperature dependence of the amplitude of the H-bond exchange contribution to reorientation.²¹ This leads to a larger activation energy overall for $\langle \tau_2 \rangle$ compared to for τ_2 (or D) that comes principally from a larger Coulombic contribution. Given the similarity between the activation energies for diffusion and reorientation we will focus on the comparisons of the former with those for $1/\eta_s$.

The results in Table I show clear qualitative similarities for the activation energy components for diffusion and viscosity. In particular, both $E_{a,D}$ and $E_{a,1/\eta_s}$ are dominated by the contribution from Coulombic interactions, which is close to the total activation energy (or $E_{a,1/\eta_s} - k_B T$ in the case of viscosity). Further, the Lennard-Jones component is negative in both cases and nearly cancels the kinetic energy contribution (though see below).

However, there are quantitative differences between the activation energy components for D and those for $1/\eta_s$. Before discussing these it is important to consider the comparisons of the decompositions in greater detail. There are two $k_B T$ terms that appear in the activation energies. First, $k_B T$ adds to the TCF-derived contribution to $E_{a,1/\eta_s}$ in Eq. 9 and, while the latter can be decomposed, the former arises within the linear response approximation. We note that it is independent of the potential present and thus is most reasonably associated with the kinetic energy component. An additional $k_B T$ must be added to $E_{a,1/\eta_s}$ to give $E_{a,D}$, Eq. 16, according to the Stokes-Einstein relation. This arises from a thermal average of the squared velocity⁵⁶ and is therefore also associated with the kinetic energy contribution. Together these two terms yield the prediction $E_{a,D}^{KE} = E_{a,1/\eta_s}^{KE} + 2k_B T$.

With this in mind, we see that $E_{a,1/\eta_s}^{KE} + 2k_B T = 2.15$ kcal/mol, which is significantly larger than the calculated $E_{a,D}$ of 1.194 kcal/mol. Similarly, there are significant differences for the Coulombic contribution, which is smaller for $E_{a,1/\eta_s}$ than for $E_{a,D}$, and the

Lennard-Jones component, which is larger for the viscosity. Interestingly, however, the total potential energy contribution to the shear viscosity activation energy, $E_{a,1/\eta_s}^{Coul} + E_{a,1/\eta_s}^{LJ} = 2.97$ kcal/mol, is the same as that for diffusion, $E_{a,D}^{Coul} + E_{a,D}^{LJ} = 3.073$ kcal/mol.

The activation energy decompositions of $E_{a,1/\eta_s}$ thus appear to not be in quantitative accord with those of $E_{a,D}$ via the Stokes-Einstein relation. The results suggest a redistribution, in translating the viscosity to diffusion, of the total potential energy contribution to the activation energy between Lennard-Jones and Coulombic interactions. Whether this is a breakdown of the Stokes-Einstein relation at a more detailed level or an effect of how H-bond exchanges are weighted in η_s versus D is not clear. If the latter, one can resolve the disagreement between the kinetic energy contributions to the activation energies by assuming, as was done above, that the effective hydrodynamic radius r (or, alternatively, the displacement distance, λ) is temperature dependent. If the resulting $\partial \ln r / \partial \beta$ term is considered as part of the $E_{a,1/\eta_s}^{KE}$ it gives a predicted kinetic energy contribution to $E_{a,D}$ of 1.29 kcal/mol, in good agreement with the calculated $E_{a,D}^{KE}$. Ultimately, these issues will be clarified by a detailed analysis, currently underway in our lab, of the fundamental process underlying both η_s and D : H-bond exchange dynamics.

VI. CONCLUSIONS

A general fluctuation theory for dynamics approach for evaluating the temperature dependence of transport coefficients *via* Green-Kubo relations has been presented and illustrated by application to the shear viscosity of water. The result is a calculation of the shear viscosity activation energy from simulations at a single temperature. The method is equivalent to taking the analytical derivative of the viscosity with respect to temperature, in contrast to the numerical derivative that is obtained from the standard Arrhenius analysis approach. While the shear viscosity is known experimentally to exhibit significant non-Arrhenius behavior,¹⁶ we find that an Arrhenius analysis is a good local approximation as it is in excellent agreement with the present direct calculation of the activation energy over a narrow 40 K temperature range.

A principal advantage of the present approach is thus that the activation energy can be decomposed into contributions from different components of the total system energy. The results show that Coulombic interactions represent the largest contributor to the $1/\eta_s$ activation energy. The Lennard-Jones term is negative, indicating that increasing this type of potential energy actually increases the shear viscosity, and effectively cancels the kinetic energy contribution. This behavior is qualitatively the same as previously observed for the activation energies associated with both diffusion¹⁹ and reorientation.^{19,21}

Three approaches to testing the Stokes-Einstein relation based on the temperature dependence of the diffusion coefficient and the viscosity have been examined and each reveals shortcomings. Namely, we find that the activation energies of D and $1/\eta_s$ do not follow the Stokes-Einstein prediction. This is also reflected, though perhaps less clearly, in the change in the ratio $D\eta_s/T$ with temperature. Finally, the decomposition of the diffusion and viscosity activation energies enabled by the fluctuation theory for dynamics approach reveals qualitative agreement in the relative Coulombic, Lennard-Jones, and kinetic energy contributions. However, there are significant quantitative differences. One potential resolution of this apparent breakdown is to consider the distance moved as a result of the H-bond exchanges in water, which relates the viscosity to the diffusion coefficient,⁵⁴ to be temperature dependent. A detailed examination of the activation energy associated with this elemental molecular process, *i.e.*, of the H-bond exchange rate constant and its contributions is needed to investigate this possibility.

ACKNOWLEDGMENTS

The authors would like to thank Professor Brian B. Laird for useful suggestions. This work was supported by the National Science Foundation under Grant No. CHE-1800559. C.H.M. gratefully acknowledges support from a Walrafen fellowship. Z.A.P. is supported by a National Science Foundation Graduate Research Fellowship under Grant Nos. 1540502 and 1451148. The calculations were performed at the University of Kansas Center for Research Computing (CRC).

APPENDIX

Here we show that, within the Stokes-Einstein approximation, the activation energies are the same for the diffusion coefficient in the infinite liquid, D , and in a periodic boundary condition simulation, D_{PBC} . The activation energy for D is given from Eq. 15 by

$$\begin{aligned} E_{a,D} &= -\frac{1}{D} \frac{\partial D}{\partial \beta} \\ &= -\frac{1}{D} \left[\frac{\partial D_{PBC}}{\partial \beta} + \frac{\partial}{\partial \beta} \left(\frac{\xi}{6\pi\beta\eta_s L} \right) \right] \\ &= \frac{D_{PBC}}{D} E_{a,D_{PBC}} \\ &\quad + \frac{\xi}{D 6\pi\beta\eta_s L} [k_B T + E_{a,1/\eta_s}], \end{aligned} \quad (18)$$

where $\xi = 2.837297$ is a constant.⁴⁷ Using Eq. 16 derived from the Stokes-Einstein relation this gives

$$E_{a,D} \left[D - \frac{\xi}{6\pi\beta\eta_s L} \right] = D_{PBC} E_{a,D_{PBC}}. \quad (19)$$

However, the term in square brackets on the left-hand-side is D_{PBC} (see Eq. 15), giving $E_{a,D} = E_{a,D_{PBC}}$.

- ¹C. Sievers, Y. Noda, L. Qi, E. M. Albuquerque, R. M. Rioux, and S. L. Scott, "Phenomena Affecting Catalytic Reactions at Solid-Liquid Interfaces," *ACS Catal.* **6**, 8286–8307 (2016).
- ²T. Kitanosono, K. Masuda, P. Xu, and S. Kobayashi, "Catalytic Organic Reactions in Water toward Sustainable Society," *Chem. Rev.* **118**, 679–746 (2018).
- ³R. Devanathan, A. Venkatnathan, and M. Dupuis, "Atomistic Simulation of Nafion Membrane. 2. Dynamics of Water Molecules and Hydronium Ions," *J. Phys. Chem. B* **111**, 13006–13013 (2007).
- ⁴K. Jiao and X. Li, "Water Transport in Polymer Electrolyte Membrane Fuel Cells," *Prog. Energy Combust. Sci.* **37**, 221–291 (2011).
- ⁵A. Warshel, P. K. Sharma, M. Kato, Y. Xiang, H. Liu, and M. H. M. Olsson, "Electrostatic Basis for Enzyme Catalysis," *Chem. Rev.* **106**, 3210–3235 (2006).
- ⁶D. Laage, T. Elsaesser, and J. T. Hynes, "Water Dynamics in the Hydration Shells of Biomolecules," *Chem. Rev.* **117**, 10694–10725 (2017).
- ⁷K. Ando and J. Hynes, "Molecular Mechanism of HCl Acid Ionization in Water: *Ab Initio* Potential Energy Surfaces and Monte Carlo Simulations," *J. Phys. Chem. B* **101**, 10464–10478 (1997).
- ⁸S. Hammes-Schiffer and A. A. Stuchebrukhov, "Theory of Coupled Electron and Proton Transfer Reactions," *Chem. Rev.* **110**, 6939–6960 (2010).
- ⁹J. T. Hynes, "Molecules in Motion: Chemical Reaction and Allied Dynamics in Solution and Elsewhere," *Annu. Rev. Phys. Chem.* **66**, 1–20 (2015).
- ¹⁰A. Einstein, *Investigations on the Theory of the Brownian Movement* (Dover, New York, 1956).
- ¹¹R. C. Tolman, "Statistical Mechanics Applied to Chemical Kinetics," *J. Am. Chem. Soc.* **42**, 2506–2528 (1920).
- ¹²D. G. Truhlar, "Interpretation of the Activation Energy," *J. Chem. Educ.* **55**, 309–311 (1978).
- ¹³L. D. Eicher and B. J. Zwolinski, "High-precision Viscosity of Supercooled Water and Analysis of the Extended Range Temperature Coefficient," *J. Phys. Chem.* **75**, 2016–2024 (1971).
- ¹⁴L. A. Woolf, "Tracer Diffusion of Tritiated Water (THO) in Ordinary Water (H₂O) under Pressure," *J. Chem. Soc., Faraday Trans. 1* **71**, 784–13 (1975).
- ¹⁵K. Krynicki, C. D. Green, and D. W. Sawyer, "Pressure and Temperature Dependence of Self-diffusion in Water," *Faraday Discuss. Chem. Soc.* **66**, 199–208 (1978).
- ¹⁶C. H. Cho, J. Urquidí, S. Singh, and G. W. Robinson, "Thermal Offset Viscosities of Liquid H₂O, D₂O, and T₂O," *J. Phys. Chem. B* **103**, 1991–1994 (1999).
- ¹⁷C. Dellago and P. G. Bolhuis, "Activation Energies from Transition Path Sampling Simulations," *Mol. Simul.* **30**, 795–799 (2004).
- ¹⁸O. O. Mesele and W. H. Thompson, "Removing the Barrier to the Calculation of Activation Energies," *J. Chem. Phys.* **145**, 134107 (2016).
- ¹⁹Z. A. Piskulich, O. O. Mesele, and W. H. Thompson, "Removing the Barrier to the Calculation of Activation Energies: Diffusion Coefficients and Reorientation Times in Liquid Water," *J. Chem. Phys.* **147**, 134103 (2017).
- ²⁰Z. A. Piskulich, O. O. Mesele, and W. H. Thompson, "Expanding the Calculation of Activation Volumes: Self-diffusion in Liquid Water," *J. Chem. Phys.* **148**, 134105 (2018).
- ²¹Z. A. Piskulich and W. H. Thompson, "The Activation Energy for Water Reorientation Differs between IR Pump-probe and NMR Measurements," *J. Chem. Phys.* **149**, 164504 (2018).
- ²²S. J. Plimpton, "Fast Parallel Algorithms for Short-Range Molecular Dynamics," *J. Comp. Phys.* **117**, 1–19 (1995).
- ²³The LAMMPS molecular dynamics package, <http://lammps.sandia.gov>.
- ²⁴J. L. F. Abascal and C. Vega, "A General Purpose Model for the Condensed Phases of Water: TIP4P/2005," *J. Chem. Phys.* **123**, 234505 (2005).
- ²⁵G. Ciccotti and J. Ryckaert, "Molecular Dynamics of Rigid Molecules," *Comp. Phys. Rep.* **4**, 346–392 (1986).
- ²⁶T. Darden, D. York, and L. Pedersen, "Particle Mesh Ewald: An $N \log(N)$ Method for Ewald Sums in Large Systems," *J. Chem. Phys.* **98**, 10089–10092 (1993).
- ²⁷E. L. Pollock and J. Glosli, "Comments on PPPM, FMM, and the Ewald Method for Large Periodic Coulombic Systems," *Comput. Phys. Comm.* **95**, 93–110 (1995).
- ²⁸R. Hockney and J. Eastwood, *Computer Simulation Using Particles*, edited by A. Hilger (Taylor and Francis, NY, 1989).
- ²⁹D. P. Shoemaker, C. W. Garland, and J. W. Nibler, *Experiments in Physical Chemistry* (McGraw-Hill, New York, 1989).
- ³⁰F. Müller-Plathe, "Reversing the Perturbation in Nonequilibrium Molecular Dynamics: An Easy Way to Calculate the Shear Viscosity of Fluids," *Phys. Rev. E* **59**, 4894–4898 (1999).
- ³¹S. Kuang and J. D. Gezelter, "A Gentler Approach to RNEMD: Nonisotropic Velocity Scaling for Computing Thermal Conductivity and Shear Viscosity," *J. Chem. Phys.* **133**, 164101 (2010).
- ³²S. Balasubramanian, C. J. Mundy, and M. L. Klein, "Shear Viscosity of Polar Fluids: Molecular Dynamics Calculations of Water," *J. Chem. Phys.* **105**, 11190–11195 (1996).
- ³³M. A. González and J. L. F. Abascal, "The Shear Viscosity of Rigid Water Models," *J. Chem. Phys.* **132**, 096101 (2010).
- ³⁴J. S. Medina, R. Prosimi, P. Villarreal, G. Delgado-Barrio, G. Winter, B. González, J. V. Alemán, and C. Collado, "Molecular Dynamics Simulations of Rigid and Flexible Water Models: Temperature Dependence of Viscosity," *Chem Phys* **388**, 9–18 (2011).
- ³⁵G. Raabe and R. J. Sadus, "Molecular Dynamics Simulation of the Effect of Bond Flexibility on the Transport Properties of Water," *J. Chem. Phys.* **137**, 104512 (2012).
- ³⁶S. Tazi, A. Boğan, M. Salanne, V. Marry, P. Turq, and B. Rotenberg, "Diffusion Coefficient and Shear viscosity of Rigid Water Models," *J. Phys.-Condens. Mat.* **24**, 284117 (2012).
- ³⁷G. S. Fanourgakis, J. S. Medina, and R. Prosimi, "Determining the Bulk Viscosity of Rigid Water Models," *J. Phys. Chem. A* **116**, 2564–2570 (2012).
- ³⁸N. Galamba, "On the Hydrogen-bond Network and the Non-Arrhenius Transport Properties of Water," *J. Phys.-Condens. Mat.* **29**, 015101 (2017).
- ³⁹T. Kawasaki and K. Kim, "Identifying Time Scales for Violation/Preservation of Stokes-Einstein Relation in Supercooled Water," *Sci. Adv.* **3**, e1700399 (2017).
- ⁴⁰P. Montero de Higes, E. Sanz, L. Joly, C. Valeriani, and F. Caupin, "Viscosity and Self-diffusion of Supercooled and Stretched Water from Molecular Dynamics Simulations," *J. Chem. Phys.* **149**, 094503 (2018).
- ⁴¹T. Yamaguchi, "Structural Origin of Shear Viscosity of Liquid Water," *J. Phys. Chem. B* **122**, 1255–1260 (2018).
- ⁴²G. Guevara-Carrion, J. Vrabec, and H. Hasse, "Prediction of Self-diffusion Coefficient and Shear Viscosity of Water and Its Binary Mixtures with Methanol and Ethanol by Molecular Simulation," *J. Chem. Phys.* **134**, 074508 (2011).
- ⁴³G. E. Walrafen and Y. C. Chu, "Shear Viscosity, Heat Capacity, and Fluctuations of Liquid Water, All at Constant Molal Volume," *J. Phys. Chem.* **95**, 8909–8921 (1991).
- ⁴⁴D. Laage and J. T. Hynes, "A Molecular Jump Mechanism of Water Reorientation," *Science* **311**, 832–835 (2006).
- ⁴⁵D. Laage and J. T. Hynes, "On the Molecular Mechanism of Water Reorientation," *J. Phys. Chem. B* **112**, 14230–14242 (2008).
- ⁴⁶B. Dunweg and K. Kremer, "Molecular Dynamics Simulation of a Polymer Chain in Solution," *J. Chem. Phys.* **99**, 6983–6997 (1993).
- ⁴⁷I.-C. Yeh and G. Hummer, "System-Size Dependence of Diffusion Coefficients and Viscosities from Molecular Dynamics Simulations with Periodic Boundary Conditions," *J. Phys. Chem. B* **108**, 15873–15879 (2004).

- ⁴⁸R. Mills, "Self-diffusion in Normal and Heavy Water in the Range 1-45°," J. Phys. Chem. **77**, 685-688 (1973).
- ⁴⁹K. R. Harris and L. A. Woolf, "Pressure and Temperature Dependence of the Self Diffusion Coefficient of Water and Oxygen-18 Water," J. Chem. Soc., Faraday Trans. 1 **76**, 377-379 (1980).
- ⁵⁰F. X. Prielmeier, E. W. Lang, R. J. Speedy, and H. D. Lüdemann, "Diffusion in Supercooled Water to 300 Mpa," Phys. Rev. Lett. **59**, 1128-1131 (1987).
- ⁵¹W. S. Price, H. Ide, and Y. Arata, "Self-Diffusion of Supercooled Water to 238 K Using PGSE NMR Diffusion Measurements," J. Phys. Chem. A **103**, 448-450 (1999).
- ⁵²K. Yoshida, N. Matubayasi, Y. Uosaki, and M. Nakahara, "Scaled Polynomial Expression for Self-Diffusion Coefficients for Water, Benzene, and Cyclohexane over a Wide Range of Temperatures and Densities," J. Chem. Eng. Data **55**, 2815-2823 (2010).
- ⁵³D. J. Wilbur, T. DeFries, and J. Jonas, "Self-Diffusion in Compressed Liquid Heavy-Water," J. Chem. Phys. **65**, 1783-1786 (1976).
- ⁵⁴S. Glasstone, K. J. Laidler, and H. Eyring, *The Theory of Rate Processes* (McGraw-Hill, New York, 1941).
- ⁵⁵D. Eisenberg and W. Kauzmann, *The Structure and Properties of Water* (Oxford, New York, 1969).
- ⁵⁶D. A. McQuarrie, *Statistical Mechanics* (HarperCollins, New York, 1976).

TOC Graphic

